Journal of Structural Geology 202 (2026) 105571

Contents lists available at ScienceDirect

Journal of Structural Geology

journal homepage: www.elsevier.com/locate/jsg

# How variations in intraplate stresses affect slip and dilation tendencies of faults: The onshore United Kingdom example

T.G. Blenkinsop

*School of Earth and Environmental Sciences, Cardiff University, Wales, CF10 3AT, United Kingdom*

A R T I C L E I N F O

*Keywords:*
Stress
Slip tendency
Dilation tendency
Fault
Intraplate
Seismic hazard

A B S T R A C T

Stresses in plate interiors vary in magnitude and orientations on various scales, implying that shear and normal stresses on faults may vary regionally. The effects of intraplate regional stress variations are analysed using a recent compilation of in-situ stress to calculate slip and dilation tendencies of United Kingdom onshore faults. The tendencies are normalised to maximum possible values. Stress in UK can be characterised by a strike slip stress field with variable orientations of maximum horizontal stress, $S_H$. Throughout southern UK, $S_H$ is orientated NW, giving rise to very low slip and dilation tendencies on NE striking Caledonian faults. North and E to ESE striking faults have very high slip tendencies, and intermediate dilation tendencies. At a major boundary in stress orientation (the Highland Boundary Fault in Scotland), $S_H$ changes abruptly to a northerly trend. Steeply dipping Caledonian faults in northern UK such as the Great Glen Fault have very high slip tendencies and intermediate dilation tendencies. Faults with low dips (e.g. the Moine Thrust) have intermediate slip and dilation tendencies. The dramatic change in slip tendencies on steeply dipping Caledonian faults from southern to northern UK illustrates some of the profound consequences of regional scale stress variations. These conclusions are robust to reasonable uncertainties, but the coarse results of this study indicate that more detailed knowledge of stress and fault geometry is necessary for applications such as pump-storage schemes, nuclear power plants, radioactive waste disposal, mining, and carbon sequestration, as well as for seismic hazard analysis.

## 1. Introduction

The interiors of plates are regions in which stress states vary over different scales (Heidbach et al., 2018; Sandiford et al., 2004; Townend and Zoback, 2000; Zoback and Zoback, 1989). The variability in scales of heterogeneity indicates that several different sources of stress are involved (Lund Snee and Zoback, 2020); among these may be gravitational potential energy and glacial rebound, in addition to stresses related to plate tectonics such as plate boundary forces and mantle drag (Levandowski et al., 2018).

Continental plate interiors are also commonly characterised by complex networks of faults on which within-plate stress states exert tractions. The relationship between the stress state and fault geometry can be expressed by slip and dilation tendencies (Moeck et al., 2009; Morris et al., 1996). Given variable stresses and networks of faults that may have evolved over many tectonic events, slip and dilation tendencies may be expected to have complex patterns, especially because fault cores link and widen with fault slip on intraplate faults (Mckay et al., 2021). These patterns are important in many engineering geology applications such as reservoirs, pump-storage schemes, nuclear power plant construction, radioactive waste disposal, mining, and geological carbon storage (e.g. Williams et al., 2018; Wiprut and Zoback, 2002), and for seismic hazard, which can be appreciable since intracontinental stress magnitudes can be large (e.g. Hillis et al., 2008; Tuttle et al., 2002). Slip and dilation tendencies are also recommended for Capable Fault Studies (e.g., ONR, 2018).

The UK exemplifies both heterogeneous intracontinental stresses and a complex fault structure (Musson, 2007). Onshore UK stresses may reflect the varying influences of the effects of the Alpine collision (Hudson and Cooling, 1988), stresses related to the Mid-Atlantic ridge (Stewart and Firth, 2000), post-glacial rebound stresses (Main et al., 1999; Muir-Wood, 2000) and the influence of hot upper mantle (Arrowsmith et al., 2005; Bott and Bott, 2004). These stresses interact with a geological framework in the UK consisting of Archean to Paleozoic basement overlain by Mesozoic-Recent sedimentary rocks (Woodcock and Strachan, 2012). The Caledonian and Variscan orogenies have had the most widespread effects in the basement, creating dominantly NE and E to SE striking faults respectively. The Caledonian

This article is part of a special issue entitled: Richard Lisle published in Journal of Structural Geology.

*E-mail address:* blenkinsopt@cardiff.ac.uk.

https://doi.org/10.1016/j.jsg.2025.105571
Received 11 August 2025; Received in revised form 29 October 2025; Accepted 5 November 2025
Available online 5 November 2025

orogeny (including the Grampian and Acadian events) dominantly affected the northern and western UK, while the effects of the Variscan orogen are most clearly expressed in the SW. Distal effects of the Pyrenean and Alpine orogenies are manifested in southern UK (Connolly et al., 2024), and evidence of extension related to the mid-Atlantic ridge and rifting in the North Sea is widespread.

Previous work in UK by Healy and Hicks (2022) analysed slip tendency and fracture susceptibility for the Porthtowan fault zone in southwestern UK and in the South Wales coalfield, and introduced a probabilistic method to include uncertainty in their analysis. Their results are consistent with observed patterns of seismicity and focal mechanisms. Despite the importance of the relationship between in-situ stress and faults, a systematic examination of slip and dilation tendencies of faults for the whole UK does not seem to have been published, unlike some countries such as Germany (Röckel et al., 2022) and Japan (Yukutake et al., 2015) and large intraplate regions e.g. southeastern Australia (Dyksterhuis and Müller, 2008). The aim of this study is to combine the latest knowledge of in-situ stresses with a fault map to assess how variations in stress may affect the slip and dilation tendencies on faults throughout onshore UK. Uncertainties are explored through a simple heuristic approach. Given the sparse knowledge of the stress field over the vast majority of UK, and the basic nature of UK-wide fault data, this can only be a preliminary and crude analysis.

## 2. Data and methods

### 2.1. UK stress field

The most comprehensive and recent analysis of the UK stress field is given in Kingdon et al. (2022). This report is an update of the worldwide compilation of in situ stress measurements in the World Stress Map 2016 (WSM2016) (Heidbach et al., 2018), increasing the amount of data from 377 to 474 and correcting some locations and quality assignments. Only A-C quality data were used, meaning that the orientation of the maximum horizontal stress $S_H$ is accurate to ±25° (Rajabi et al., 2025), and these were interpolated onto a 0.1° grid (Ziegler and Heidbach, 2019) (Fig. 1).

To calculate the slip and dilation tendencies, the orientations of the principal stresses and their relative magnitudes are required. Relative magnitudes of stresses are given by Bishop's ratio (e.g. Lisle and Orife, 2002)

$$\Phi = \frac{\sigma_2 - \sigma_3}{\sigma_1 - \sigma_3}$$

Where $\sigma_1 \geq \sigma_2 \geq \sigma_3$ are the magnitudes of the principal stresses with compression positive. Values of Φ from 20 measurements in UK from WSM2016 are variable. The average is 0.445 (Fig. 2), and there are no geographical trends. Baptie (2010) found values of 0.44–0.5 for England and 0.9–0.97 for Scotland. The 0.445 value assumed here is within the range estimated by Gamboa et al. (2019) and Williams et al. (2018). The latter authors found that Φ varied slightly with depth between 0.342 at 1 km and 0.551 at 10 km in the Irish Sea Basin.

In Kingdon et al. (2022), 59 % of the data were strike slip solutions, with 24 % normal and 17 % reverse. In the Irish Sea Basin, all stress types were strike slip. A strike slip stress type was inferred by Chadwick et al. (1996) for UK; it is the most common focal mechanism for British earthquakes studied by Baptie (2010), and it is also inferred by Healy and Hicks (2022). No regional trends for stress type can be identified, and in some cases, different stress types are recorded at the same location. A strike slip stress type has been assumed here, with horizontal maximum and minimum principal stresses, and $S_H$ at the interpolated azimuth from Kingdon et al. (2022).

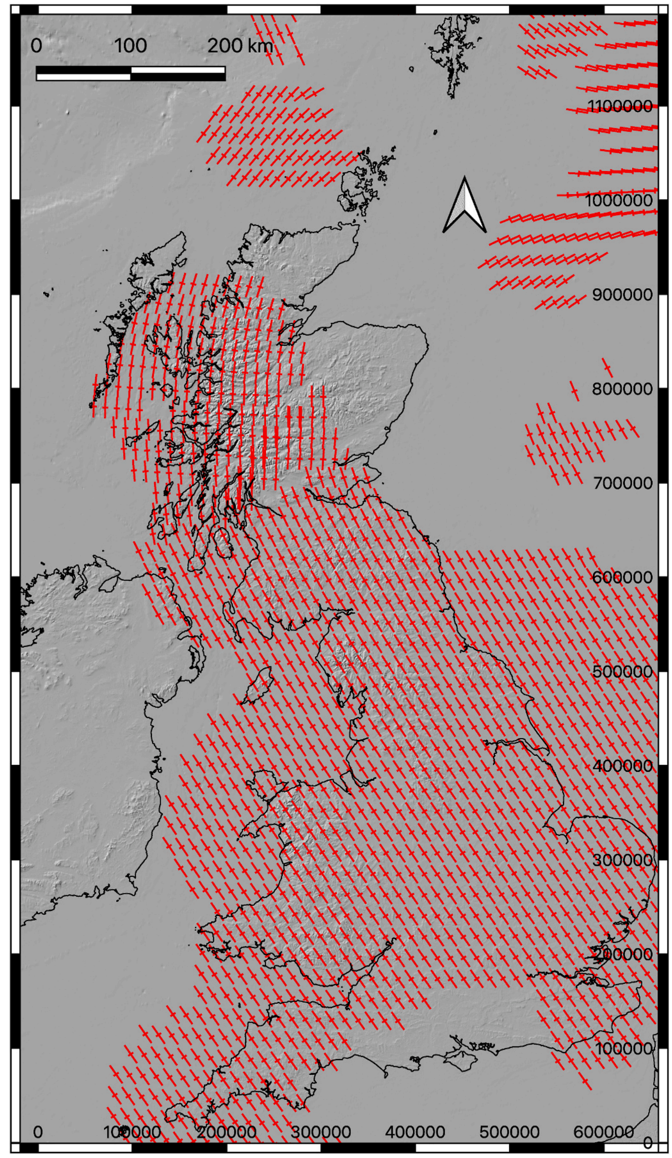


**Fig. 1.** Azimuth of the maximum horizontal stress $S_H$ in UK (red bars) from Kingdon et al. (2022). Values have been interpolated onto a 0.1° grid. (For interpretation of the references to colour in this figure legend, the reader is referred to the Web version of this article.)

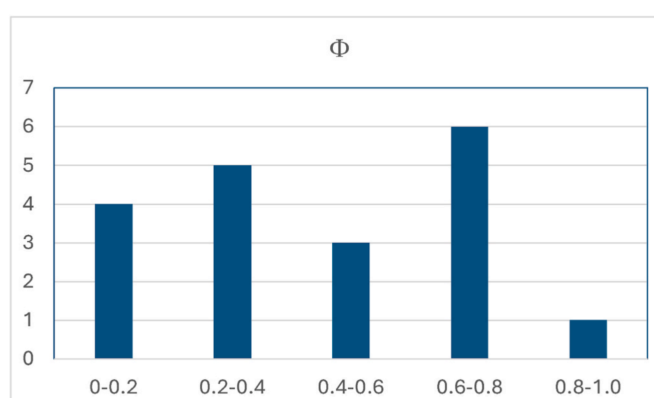


**Fig. 2.** Histogram of Bishop's ratio Φ from 19 determinations in the WSM 2016 database in the UK ((Heidbach et al., 2018).

### 2.2. Fault database

The national dataset of UK faults at 1:625000 (https://www.bgs.ac.uk/datasets/bgs-geology/) maps 2741 faults with 37264 vertices spaced from 2 m to 16 km, an average segment length of 912 m and an average of 14 vertices/fault. Faults identified as thrusts were assigned a dip of 30°: otherwise, they were treated as vertical, and the sensitivity of the analysis to these assumptions is tested.

### 2.3. Slip and dilation tendency

Morris et al. (1996) defined the Slip Tendency $T_S$ as:

$$T_S = \tau / \sigma_n \quad (1)$$

where $\tau$ is shear stress and $\sigma_n$ is normal stress. Subsequently Lisle and Srivastava (2004) defined a *normalised slip tendency* $T'_S$ as:

$$T'_S = T_S / max\ T_S = \tau / \sigma_n \tan \theta \quad (2)$$

where $\theta$ is the angle of internal friction, which for many rocks can be approximated as 30°, as used initially in this study. Lisle and Srivastava (2004) showed how $T'_S$ can be expressed entirely in terms of the orientation of the fault with respect to the principal stresses, the ratio between the principal stresses $\Phi$ and the angle of friction $\theta$, by assuming that the state of stress was such that failure occurs on the optimally orientated fault, for which $T'_S = 1$.

The dilation tendency $T_D$ is defined (e.g. Moeck et al., 2009) as:

$$T_D = (\sigma_1 - \sigma_n) / (\sigma_1 - \sigma_3) \quad (3)$$

Thus defined, $T_D$ varies from 0 to 1 for fractures with normal stresses of $\sigma_1$ and $\sigma_3$ respectively. However, this measure has limited use for stress analysis, since it requires estimates of the magnitudes of the principal stresses, which are rarely determined. To normalise the dilation tendency, the most favourable orientation of fracture is taken to be dilating (by assuming $\sigma_3 = 0$), allowing the *normalised dilation tendency* $T'_D$ to be calculated as a function only of fracture orientation, stress orientation, and Bishop's ratio. This simplification of the problem is analogous to the step taken by Lisle and Srivastava (2004) for normalising slip tendency, when they assumed that a failure criterion was met for the most favourably orientated fault.

The principal stress orientations on each fault segment were taken as the nearest values from the 0.1° grid from Kingdon et al. (2022). These were used to calculate the normalised slip and dilation tendencies on every fault segment. An advantage of defining normalised slip and dilation tendencies as above is that they are independent of the pore fluid pressure, which is generally poorly known. These measures are therefore not criteria for shear or dilatant reactivation. For convenience all slip and dilation tendencies referred to hereafter will be the normalised values.

## 3. Results

### 3.1. Stress field

The interpolated stress field (Fig. 1) shows that the stress field in UK is markedly heterogenous. South of the Highland Boundary Fault in Scotland, in all of England, Wales, Northern Ireland, the Southern Uplands and the Midland valley, $S_H$ is orientated at about 325°. At the Highland Boundary Fault there is an abrupt change to a N trend, which rotates progressively clockwise to become NE towards northern Scotland.

### 3.2. Slip and dilation tendencies

Figs. 3 and 4 show the normalised slip and dilation tendencies for all faults from the database. There are some striking patterns, which can be divided into 6 groups for the purpose of describing the results. In the strike slip stress field of UK, vertical planes at 30° to $S_H$ will have maximum slip tendencies; vertical planes in the direction of $S_H$ will have maximum dilation tendencies.

1. The Moine Thrust Zone and Outer Isles Thrusts in NW Scotland.

These and related faults strike NNE and dip to the ESE. Although they have a low angle to $S_H$, their 30° dip means that they have low-intermediate slip tendencies, but intermediate to high dilation tendencies.

2. The Great Glen and Highland Boundary Faults in northern Scotland.

As well as the Great Glen and Highland Boundary Faults, this group includes the Helmsdale, Strathglass, Ericht-Laidon, and the Tyndrum Faults. These faults strike generally NE and make an angle of about 30° to the N trending $S_H$. They are therefore in an ideal orientation for reactivation and have very high slip tendencies. Their dilation tendencies are variable and depend sensitively on strike: more northerly strikes have high normalised dilation tendencies, while more easterly strikes have low dilation tendencies.

3. NE striking faults south of the Highland Boundary Fault.

These faults are strongly expressed in the Southern Uplands (examples include the Southern Uplands, Leadhills, Fardingmullah, and Orloch Bridge Faults) and Northern Ireland but also occur sporadically in northern England. In Wales, examples include the Carreg Cennen Disturbance-Church Stretton fault, the Swansea Valley and Neath Disturbances, the Menai Straights Fault System, and the Welsh borderland fault system. In contrast to the previous group of faults, which have similar strikes, these faults have very low slip and dilation tendencies, because they are approximately perpendicular to $S_H$.

4. N striking faults in the England and Wales.

There are many N striking faults throughout England and Wales, including for example the Frankby and Woodchurch Faults, which are within a high-density area of such faults in northeastern England. Parts of the Pennine and Dent Faults that lie on the edge of the Carboniferous fault blocks of northern England are included. The group extends to the S to include the Malvern Fault. These faults are at the optimal orientation to $S_H$ and show maximum values of slip tendencies, and high dilation tendencies.

5. NNW to NW striking faults.

These occur in the Southern Uplands, Northern Ireland, NE England, Wales and SW England, where examples include the Porthtowan fault, the Sticklepath-Lustleigh Fault and the Cambeek Cawsand Fault Zone. A few examples can be found in eastern and southern England and Scotland. They have low slip tendencies in southern UK because they are sub-parallel to $S_H$. Where they occur with Caledonian faults, such as in South Wales and the Southern Uplands, they are perpendicular to these faults, which they abut, and both groups of faults have low slip tendencies because they are parallel to principal planes of stress. These faults have intermediate to high slip tendencies N of the Highland Boundary Fault. They have maximum dilation tendencies in southern UK, but low dilation tendencies N of the Highland Boundary Fault.

6. E to ESE striking faults of England and Wales

Theses faults occur throughout England and Wales, including the Stublick Fault, the Dent Fault and the Flanborough Head Fault, and most of the faults in southeastern England. The Benton Fault in Wales, and the

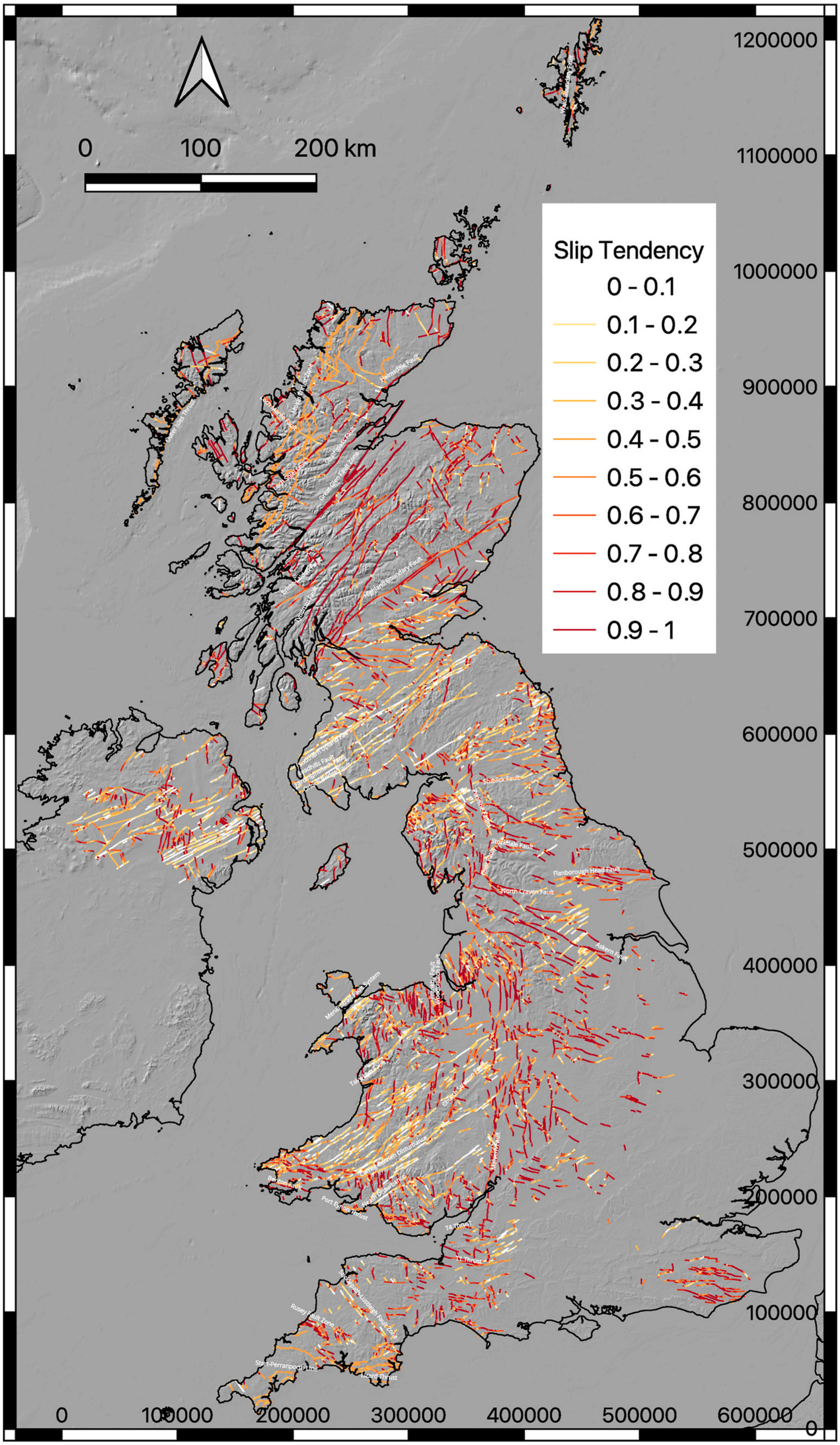


**Fig. 3.** Normalised slip tendency calculated on fault segments from the nearest interpolated stress determination. The background to this figure and Figs. 4, 5 and 7 is hill-shaded SRTM15+ topography and bathymetry (Tozer et al., 2019). OSGB36/British National Grid coordinate reference system.

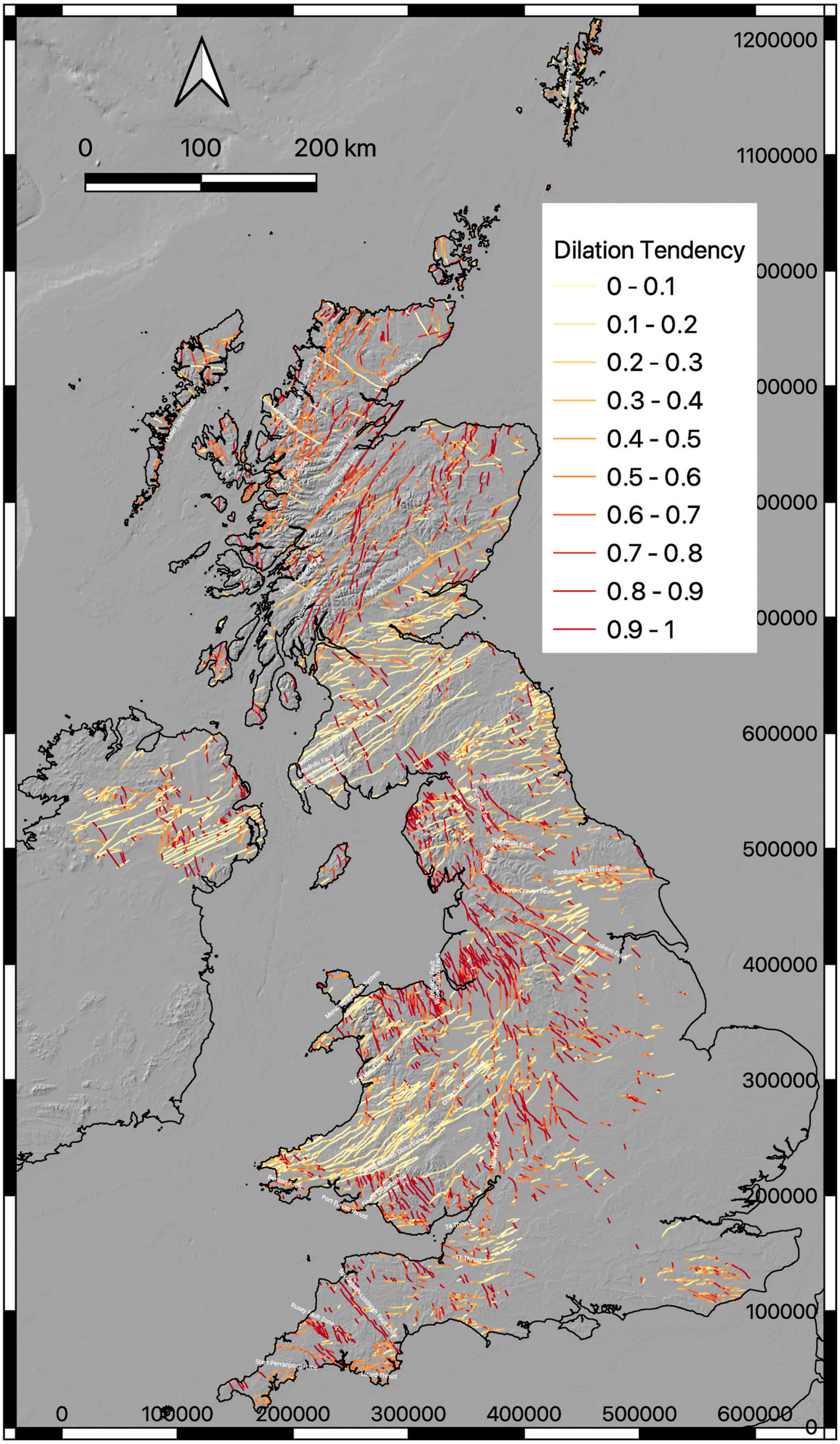


**Fig. 4.** Normalised dilation tendency calculated on fault segments from the nearest interpolated stress determination.

Sticklepath-Lustliegh Fault Zone and the Rusey Fault in southwestern England, are other examples. Because of their acute angle to $S_{H,}$ they have very high slip tendencies. A subset of faults in this group is Variscan thrusts, such as the Port Eynon fault in South Wales, some faults of the Bristol-Mendip Foreland Thrust Belt, the Lizard thrust, and the Start-Perranporth line (the Carrick Thrust) in southwestern England. They have low to intermediate slip tendencies and intermediate to high dilation tendencies.

### 3.3. Summary

A generalised map of the above results is shown in Fig. 5, while Fig. 6 shows the slip and dilation tendencies on stereoplots. A striking result is the change from very low values of slip tendency on NE striking faults south of the Highland Boundary Fault, to very high values on similar orientated faults to the N. This can be mostly attributed to the change in azimuth of $S_H$ across the Highland Boundary Fault (Fig. 1), but there is also a slight change in the orientation of these Caledonian faults. Together these factors cause the angle between the faults and $S_H$ to reduce from about 90° to the optimum value for high slip tendencies. Results for dilation tendency are generally comparable with slip tendencies, although the Caledonian faults have lower dilation tendencies N of the Highland Boundary Fault. Similarly, E to ENE and N striking fault dilation tendencies are generally somewhat lower than their slip tendencies. By contrast, NW striking faults such as the Sticklepath-Lustleigh Fault have much higher dilation than slip tendencies in southern UK: this relationship reverses N of the Highland Boundary Fault.

## 4. Discussion

The fault database imposes limitations on the detail possible in this study. The calculated slip and dilation tendencies are subject to four other sources of uncertainty: the in-situ stress, the distances between the interpolated stress locations and the fault segments, fault dips, and the angle of internal friction.

### 4.1. The fault database

The fault database is constrained by the nominal scale of mapping (1:625 000) which inevitably leads to simplifications and omissions. These only allow the regional scale of analysis as attempted here. There is a notable paucity of mapped faults in the southeast of England. Aldiss (2013) has commented that for the London region, faults are under-represented because of past mapping methods, uniformity of bedrock units, widespread Quaternary and anthropogenic deposits and urban development. Some of these factors probably apply over a larger region.

### 4.2. In situ stress

The 474 stress measurements used to generate the interpolated field are reasonably well distributed in Wales and central England, but sparse in southern England, Scotland and Northern Ireland (Kingdon et al., 2022). Nevertheless, there is a clear division of the UK stress field: England, Wales, Northern Ireland and Scotland to the south of the Highland Boundary Fault, have a very homogenous stress field with $S_H$ trending NW, agreeing with previous analyses (e.g. Baptie, 2010). The interpolation of Carafa and Barba (2013) shows slightly more variation because of a different interpolation algorithm, but is based on the more limited data of the 2008 version of the world stress map.

Stress states to the N of the Highland Boundary Fault are less well constrained by the data and more heterogenous: the trend of $S_H$ rotates clockwise with increasing latitude. The value for Bishop's ratio may also be different here (Baptie, 2010). The cause of the change in the stress field across the Highland Boundary Fault is not known. High values of post-glacial rebound in Scotland may indicate that stresses related to this factor are more important (Baptie, 2010). Post-glacial stress changes are thoroughly discussed by Stewart and Firth (2000), who conclude that the roles of tectonic stress and glacial rebound stresses cannot be distinguished. The change in orientation of $S_H$ is apparently very abrupt at the Highland Boundary Fault (Fig. 1), perhaps implying that crustal structure plays a role. Such abrupt changes in intracontinental stress

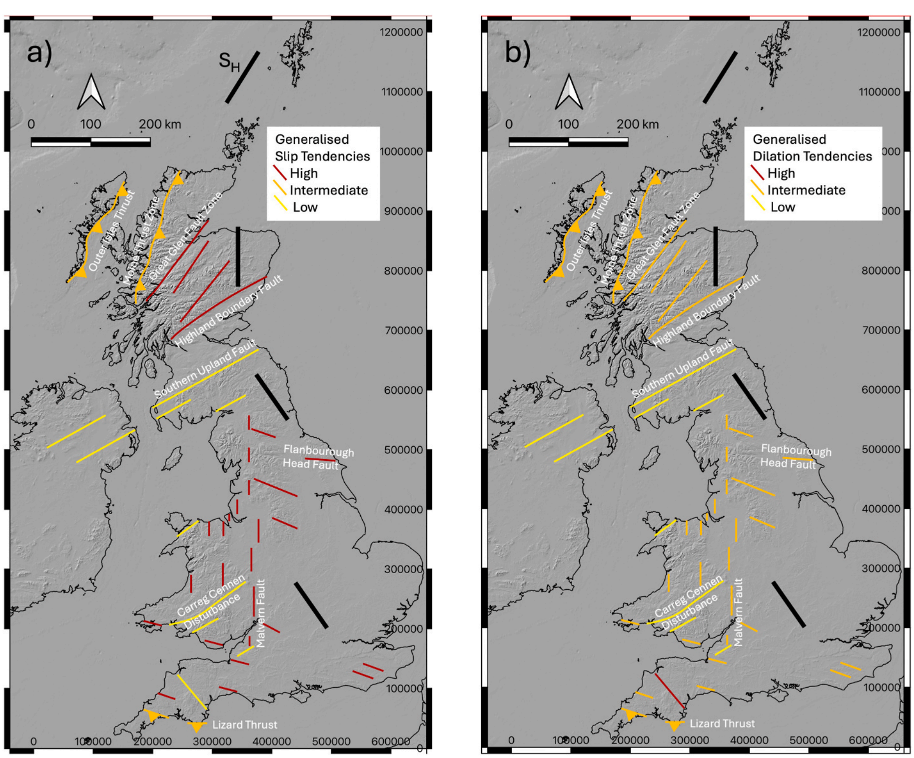


**Fig. 5.** Generalised synthesis of results a) Normalised slip tendency b) Normalised dilation tendency.

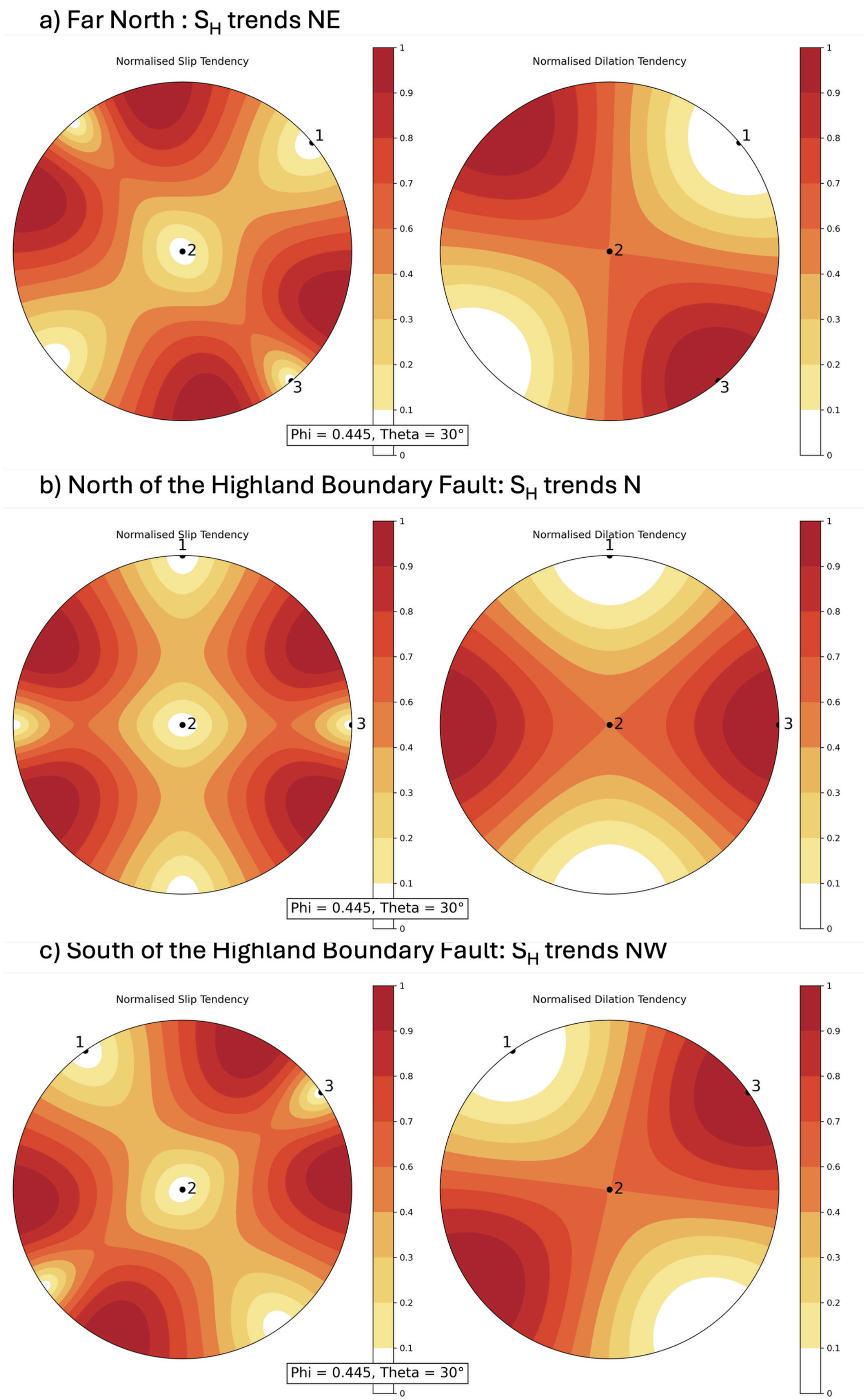


**Fig. 6.** Normalised slip and dilation tendencies plotted at poles to planes on lower hemisphere, equal area stereoplots. Principal stresses $\sigma_1$, $\sigma_2$, $\sigma_3$ labelled 1, 2, 3.

field are known elsewhere, where they have been attributed to shallow sources of stress, such as density variations in the upper crust (Lund Snee and Zoback, 2020). This explanation appears to contrast with one based on the role of lithospheric thickness variations in controlling intraplate seismicity and strength (Bonadio et al., 2025).

To evaluate the effect of uncertainty in the orientation of $S_H$, slip and dilation tendencies were also calculated on every fault segment for $S_H$ perturbed by $\pm 20^\circ$ (Table 1). This value was selected because it is the uncertainty in B quality stress determinations in WSM2016 (Rajabi et al., 2025).

The calculated slip and dilation tendencies are sensitive to the azimuth of $S_H$. Variations of $\pm 20^\circ$ cause average differences of 0.3 and 0.2 in slip and dilation tendencies respectively. Nevertheless, the overall patterns of slip tendency and dilation tendency, and the profound differences in $T'_S$ and $\Delta T'_D$ in faults from the N to the S of UK, persist when $S_H$ azimuths are perturbed.

Bishop's ratio is not well constrained by the in-situ stress data. However, variations in the ratio have a minor effect on the calculated slip and dilation tendencies. Table 2 shows statistics of the absolute difference between the slip and dilation tendencies calculated for every segment using the average value of the ratio (0.445) and those calculated using values of 0.345 and 0.545 (differing by $\pm$ 0.1 from the average values). The average absolute difference is only on the order of 0.01, or 1 % of the range of possible $\Phi$ values.

### 4.3. Distance to interpolated stress location

The distance from a fault segment to the nearest interpolated stress location varies from 121 m to 115 km, with an average of 15 km (Fig. 7). Three areas have particularly large values: The Shetland Isles, northern Scotland, and the eastern part of Northern Ireland. Slip and dilation tendency results for these areas should be treated with caution due to the large distance from interpolated stress measurements.

### 4.4. Effect of variations in fault dip

The sensitivity of slip and dilation tendencies to fault dip was analysed by comparing these quantities calculated for dips of 10° and 20° less than the values assumed initially (30° for thrusts and 90° for all other faults) (Table 3).

Average differences from the reference values reach 0.1017, or about 10 %, for dips that are 20° less than assumed: the results are not very sensitive to reasonable uncertainties in dip, which can also be inferred from Fig. 6.

### 4.5. Effect of varying angle of internal friction

The angle of internal friction $\theta$ was varied from the reference value of 30° to a lower value of 20° and a higher value of 40°. Table 4 shows the absolute differences of slip and dilation tendencies for these cases compared to those calculated from the reference value.

These variations in $\theta$ change the average slip and dilation tendencies by up to 6 %. Again, the results are robust, given conventional estimates and reasonable uncertainties in this parameter. These values may need to be lowered if the "weak fault in strong crust" model is applicable (e.g. Copley, 2018).

**Table 1**
Effect of varying the azimuth of $S_H$ on the slip and dilation tendency of fault segments. $\Delta T'_S$, $\Delta T'_D$: absolute value of the difference between the slip and dilation tendencies based on $S_H$ from Kingdon et al. (2022), and the tendencies calculated for perturbed orientations of $S_H$.

| | $S_H$+20° | | $S_H$-20° | |
|---|---|---|---|---|
| | $\Delta T'_S$ | $\Delta T'_D$ | $\Delta T'_S$ | $\Delta T'_D$ |
| Average | 0.3053 | 0.1867 | 0.2931 | 0.1977 |
| Maximum | 0.9109 | 0.3506 | 0.9111 | 0.3503 |
| Minimum | 0.0000 | 0.0000 | 0.0000 | 0.0000 |
| Standard Deviation | 0.2099 | 0.1122 | 0.2009 | 0.1135 |

**Table 2**
Effect of varying Bishop's ratio $\Phi$ on the slip and dilation tendency of fault segments. $\Delta T'_S$, $\Delta T'_D$: absolute value of the difference between the reference slip and dilation tendency statistics calculated for $\Phi = 0.445$ and those calculated for the indicated values of $\Phi$.

| | $\Phi = 0.345$ | | $\Phi = 0.545$ | |
|---|---|---|---|---|
| | $\Delta T'_S$ | $\Delta T'_D$ | $\Delta T'_S$ | $\Delta T'_D$ |
| Average | 0.0098 | 0.0116 | 0.0112 | 0.0116 |
| Maximum | 0.0900 | 0.0776 | 0.1034 | 0.0774 |
| Minimum | 0.0000 | 0.0000 | 0.0000 | 0.0000 |
| Standard Deviation | 0.0161 | 0.0246 | 0.0200 | 0.0246 |

**Table 3**
Effect of varying fault dip on the slip and dilation tendency of fault segments. $\Delta T'_S$, $\Delta T'_D$: absolute value of the difference between the slip and dilation tendency statistics for dips of 30° for thrusts and 90° for all other faults, and those calculated for dips of 10° and 20° less.

| | Dip-10° | | Dip-20° | |
|---|---|---|---|---|
| | $\Delta T'_S$ | $\Delta T'_D$ | $\Delta T'_S$ | $\Delta T'_D$ |
| Average | 0.0403 | 0.0144 | 0.1017 | 0.0429 |
| Maximum | 0.2576 | 0.0743 | 0.4489 | 0.1223 |
| Minimum | 0.0000 | 0.0000 | 0.0000 | 0.0000 |
| Standard Deviation | 0.0479 | 0.0136 | 0.0950 | 0.0239 |

**Table 4**
Effect of varying the angle of internal friction on the slip and dilation tendency of fault segments. $\Delta T'_S$, $\Delta T'_D$: absolute value of the difference between the reference slip and dilation tendency statistics ($\theta = 30^\circ$) and those calculated for $\theta =$ 20° and 40°.

| | $\theta = 20$ | | $\theta = 40$ | |
|---|---|---|---|---|
| | $\Delta T'_S$ | $\Delta T'_D$ | $\Delta T'_S$ | $\Delta T'_D$ |
| Average | 0.0550 | 0.0019 | 0.0619 | 0.0019 |
| Maximum | 0.1143 | 0.0091 | 0.1279 | 0.0091 |
| Minimum | 0.0000 | 0.0000 | 0.0000 | 0.0000 |
| Standard Deviation | 0.0308 | 0.0021 | 0.0331 | 0.0021 |

### 4.6. Implications for seismic hazard

Although UK is considered as a "low seismicity" area (Mosca et al., 2022), there is nevertheless a significant seismic record dating back to 7th Century AD (Musson, 1997), including some notable natural and induced seismic events, which have caused damage and injury (Foulger et al., 2018). Some natural seismicity in the UK is the result of reactivation of structures (Musson, 2012). Larger magnitude induced UK seismic events can also be attributed to reactivation (Clarke et al., 2014; Davies et al., 2013). Chadwick et al. (1996) have defined seismotectonic zones for UK: For example, in southern UK, seismicity is associated with distributed reactivation of Variscan and Caledonian faults, and in northern UK seismicity is associated with major NE striking faults and fault intersections with the Moine Thrust. Interactions between blocks may be important in controlling seismicity (Chadwick et al., 1996; Musson and Sargeant, 2007). These studies provide a background and a rationale for analysing slip and dilation tendencies of UK faults in the context of seismicity.

As an intraplate area with low levels of seismicity and no observed surface fault breaks from natural earthquakes, locations of earthquakes in UK are mostly not accurate enough to attribute them to specific faults (Musson, 1997). Few moment tensors have been produced for UK earthquakes (Baptie, 2010), adding to the difficulty of attributing specific earthquakes to geological examples. As an example, Fig. 8 shows seismicity and slip tendency from the BGS catalogue in the Menai straights/Llŷn peninsula area, a notable concentration of seismicity in north Wales, and the area of highest seismic hazard in UK (Baptie, 2021). The longest faults strike NE, parallel to the Menai Straights Fault System. Although some epicentres are on or close to these faults, there is no marked alignment of epicentres with the faults, which have low slip tendencies. By contrast, N and ESE striking faults in the area have very high slip tendencies (Fig. 8). The high density of events on the Llŷn peninsula (around events 4 and 5 inFig. 8) relate to the Llŷn earthquake of 1984. Aftershocks of this event define a sub-vertical plane striking ESE (Baptie, 2010; Lisle, 1992; Marrow and Walker, 1988; Trodd et al., 1985), which would have a very high slip tendency. Events 10 and 19 both have sub-vertical N striking planes, potentially reactivated in the

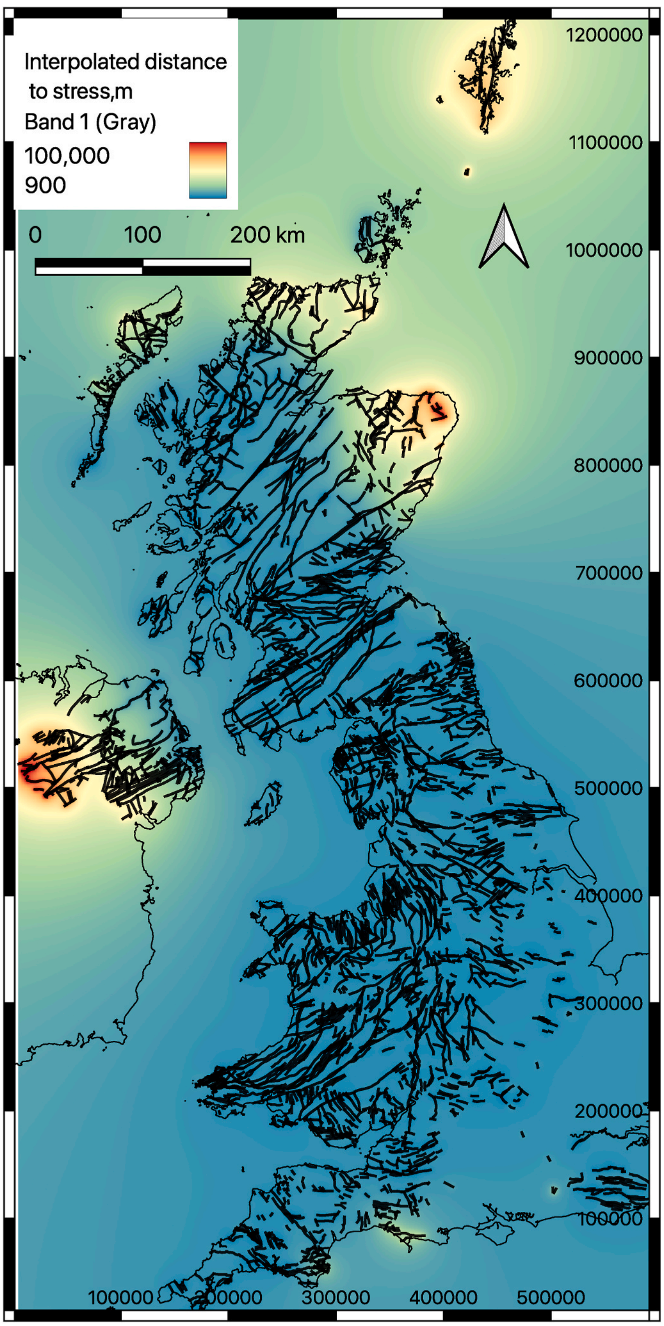


**Fig. 7.** Distance (m) from nearest interpolated stress determination (as seen in Fig. 1).

NW trending $S_H$ stress field (cf. Blenkinsop et al., 1986).

The concept of the critically stressed crust (Townend and Zoback, 2000) may apply to the relation between seismicity and structure in the UK. In intraplate regions, faulting may prevent pore fluid pressures rising above hydrostatic, as suggested by measurements in UK and in Europe, U.S.A. and Russia (Table 1 in Townend and Zoback, 2000). The occurrence of induced seismicity is another hallmark of critically stressed crust: 17 instances of human-induced earthquakes are known in UK, from mining, enhanced geothermal systems, fracking, construction and conventional oil and gas operations (Foulger et al., 2018). Critically stressed crust should fail preferentially on faults with high slip tendencies. However, a relation between seismicity and faults may not be evident at the coarse scale of Figs. 3 and 4, which are simplified representations of the UK fault network, and do not have much information about faults at depth. Another factor that may complicate the relationship between seismicity and stress is the possibility of seismicity in damage zones (e.g. Ault et al., 2015; Powers and Jordan, 2010), which may be important in assessing hazard for underground storage and geothermal energy (Peacock et al., 2025).

Because of the caveats mentioned above, the maps shown in Figs. 3 and 4 are of limited direct use in seismic hazard, especially for specific sites, which will need more detailed characterisation of both the stress field and fault geometry than in this preliminary analysis (ONR, 2018). More sophisticated, probabilistic, methods such as those of Healy and Hicks (2022) are also necessary for detailed studies. The maps show patterns which can be applied to other faults that are mapped in greater detail, as they show how the slip and dilation tendencies vary regionally. It is interesting to note that an enhanced slip tendency analysis is possible in Germany (Röckel et al., 2022) because of more detailed knowledge of the stress field, including its variation with depth and accounting for pore fluid pressure, and because three-dimensional fault geometries are known in some detail for major faults. There are regional ($\geq$100 km) scale variations in stress orientations in Germany comparable to the scale of those observed in UK.

## 5. Conclusions

Heterogeneous intraplate stresses affect a typically complex continental fault infrastructure in UK. Throughout England, Wales, Northern Ireland and southern Scotland, $S_H$ is orientated NW. In these areas, NE striking faults are perpendicular to $S_H$ and have very low slip and dilation tendencies; N and E to ESE faults at moderate angles to $S_H$ have very high slip tendencies, and intermediate dilation tendencies. At and N of a major change in the intraplate stress field at the Highland Boundary Fault, $S_H$ trends N, turning to NE in the far north of Scotland. Steeply dipping NE striking faults such as the Great Glen Fault have very high slip tendencies and intermediate dilation tendencies. Gently dipping NE striking faults such as the Moine Thrust have intermediate slip and dilation tendencies. These and other patterns of slip and dilation tendencies are markedly different from southern to northern UK.

Stress measurements are distributed unevenly across UK, giving rise to uncertainties in the orientation of $S_H$ and Bishop's ratio. Distances from faults to interpolated stress measurements are many kilometres in Northern Ireland, N and NE Scotland. Few fault geometries are well known below surface, and there is also uncertainty in the coefficient of friction. Analysis of these uncertainties suggests that the results are sufficiently robust to conclude that variation of in-situ stress within the UK causes major changes in slip and dilation tendency across UK onshore faults. These deficiencies in knowledge about stress and fault geometry need to be addressed urgently as use of the subsurface for underground storage, and nuclear plant construction and waste disposal, are becoming increasing priorities.

## Data statement

A database of the calculated slip and dilation tendencies is available

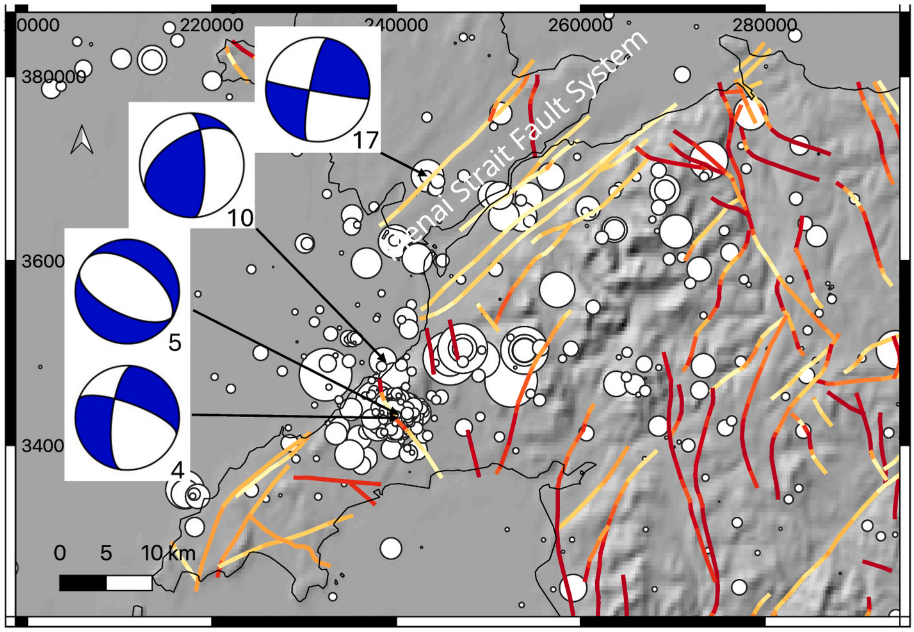


**Fig. 8.** Detail of the Menai Straights/Llŷn peninsula area, show slip tendencies on faults, and all epicentres extracted from the BGS seismicity catalogue (https://www.earthquakes.bgs.ac.uk/earthquakes/dataSearch.html), scaled by ML. Focal mechanism solutions and labels from Baptie (2010) plotted using Obspy (https://docs.obspy.org/) (Beyreuther et al., 2010).

at: https://github.com/tblenkinsop/Slip-and-Dilation-Tendencies.

## Declaration of competing interest

The authors declare that they have no known competing financial interests or personal relationships that could have appeared to influence the work reported in this paper.

## Acknowledgements

This study was inspired by reflections on Richard Lisle and his contributions to structural geology. Bob Holdsworth's review led to greater circumspection about the significance of the results, and, together with those of an anonymous reviewer, other helpful improvements.

This is Cardiff EARTH CRediT Contribution 50.

## Data availability

Data is available from Github.

## References

Aldiss, D.T., 2013. Under-representation of faults on geological maps of the London region: reasons, consequences and solutions. PGA (Proc. Geol. Assoc.) 124, 929–945. https://doi.org/10.1016/j.pgeola.2013.03.001.

Arrowsmith, S.J., Kendall, M., White, N., VanDecar, J.C., Booth, D.C., 2005. Seismic imaging of a hot upwelling beneath the British isles. Geology 33, 345–348. https://doi.org/10.1130/G21209.1.

Ault, A.K., Reiners, P.W., Evans, J.P., Thomson, S.N., 2015. Linking hematite (U-Th)/He dating with the microtextural record of seismicity in the wasatch fault damage zone, Utah, USA. Geology 43, 771–774. https://doi.org/10.1130/G36897.1.

Baptie, B., 2021. Earthquake Seismology 2020/2021 BGS. British Geological Survey Open Report. OR/21/033 42pp.

Baptie, B., 2010. Seismogenesis and state of stress in the UK. Tectonophysics 482, 150–159. https://doi.org/10.1016/j.tecto.2009.10.006.

Beyreuther, M., Barsch, R., Krischer, L., Behr, Y., Wasserman, J., 2010. ObsPy: a python toolbox for seismology. Seismol Res. Lett. 81, 530–533.

Blenkinsop, T.G., Long, R.E., Kusznir, N.J., Smith, M.J., 1986. Seismicity and tectonics in Wales. J Geol Soc London 143. https://doi.org/10.1144/gsjgs.143.2.0327.

Bonadio, R., Lebedev, S., Chew, D., Xu, Y., Fullea, J., Meier, T., 2025. Volcanism and long-term seismicity controlled by plume-induced plate thinning. Nat. Commun. 16. https://doi.org/10.1038/s41467-025-62967-5.

Bott, M.H.P., Bott, J.D.J., 2004. The Cenozoic uplift and earthquake belt of mainland britain as a response to an underlying hot, low-density upper mantle. J. Geol. Soc. 161, 19–29. London.

Carafa, M.M.C., Barba, S., 2013. The stress field in Europe: optimal orientations with confidence limits. Geophys. J. Int. 193, 531–548. https://doi.org/10.1093/gji/ggt024.

Chadwick, R.A., Pharaoh, T.E., Williamson, J.P., Musson, R.M.W., 1996. Seismotectonics of the UK. BGS Technical Report WA/96/3C: Issue 1.0.

Clarke, H., Eisner, L., Styles, P., Turner, P., 2014. Felt seismicity associated with shale gas hydraulic fracturing: the first documented example in Europe. Geophys. Res. Lett. 41, 8308–8314. https://doi.org/10.1002/2014GL062047.

Connolly, J., Anderson, M., Mottram, C., Price, G.D., Parrish, R., Sanderson, D., 2024. Using U–Pb carbonate dating to constrain the timing of extension and fault reactivation within the Bristol channel basin, SW England. J Geol Soc London 181. https://doi.org/10.1144/jgs2024-021.

Copley, A., 2018. The strength of earthquake-generating faults. J Geol Soc London 175, 1–12. https://doi.org/10.1144/jgs2017-037.

Davies, R., Foulger, G., Bindley, A., Styles, P., 2013. Induced seismicity and hydraulic fracturing for the recovery of hydrocarbons. Mar. Petrol. Geol. 45, 171–185. https://doi.org/10.1016/j.marpetgeo.2013.03.016.

Dyksterhuis, S., Müller, R.D., 2008. Cause and evolution of intraplate orogeny in Australia. Geology 36 (1), 495–498. https://doi.org/10.1130/G24536A.

Foulger, G.R., Wilson, M.P., Gluyas, J.G., Julian, B.R., Davies, R.J., 2018. Global review of human-induced earthquakes. Earth Sci. Rev. 176, 438–514. https://doi.org/10.1016/j.earscirev.2017.07.008.

Gamboa, D., Williams, J.D.O., Bentham, M., Schofield, D.I., Mitchell, A.C., 2019. Application of three-dimensional fault stress models for assessment of fault stability for CO2 storage sites. Int. J. Greenh. Gas Control 90. https://doi.org/10.1016/j.ijggc.2019.102820.

Healy, D., Hicks, S.P., 2022. De-risking the energy transition by quantifying the uncertainties in fault stability. Solid Earth 13, 15–39. https://doi.org/10.5194/se-13-15-2022.

Heidbach, O., Rajabi, M., Cui, X., Fuchs, K., Müller, B., Reinecker, J., Reiter, K., Tingay, M., Wenzel, F., Xie, F., Ziegler, M.O., Zoback, Mary Lou, Zoback, Mark, 2018. The world stress map database release 2016: crustal stress pattern across scales. Tectonophysics. https://doi.org/10.1016/j.tecto.2018.07.007.

Hillis, R.R., Sandiford, M., Reynolds, S.D., Quigley, M.C., 2008. Present-Day Stresses, Seismicity and neogene-to-recent Tectonics of Australia's 'Passive' Margins: Intraplate Deformation Controlled by Plate Boundary Forces, 306. Geological Society, London, Special Publications, pp. 71–90.

Hudson, J.A., Cooling, C.M., 1988. In situ rock stresses and their measurement in the U. K.—part I. The current state of knowledge. Int. J. Rock Mech. Min. Sci. Geomech. Abstracts 25, 363–370. https://doi.org/10.1016/0148-9062(88)90976-X.

Kingdon, A., Williams, J., Fellgett, M., Rettelbach, N., Heidbach, O., 2022. Stress map of Great Britain and Ireland 2022. QFZ Data Services, GFZ German Research Center for Geosciences. https://doi.org/10.5880/WSM.GreatBritainIreland2022.

Levandowski, W., Herrmann, R.B., Briggs, R., Boyd, O., Gold, R., 2018. An updated stress map of the continental United States reveals heterogeneous intraplate stress. Nat. Geosci. 11, 433–437. https://doi.org/10.1038/s41561-018-0120-x.

Lisle, R.J., 1992. New method of estimating regional stress orientations: application to focal mechanism data of recent British earthquakes. Geophys. J. Int. 110, 276–282.
Lisle, R.J., Orife, T., 2002. STRESSTAT: a basic program for numerical evaluation of multiple stress inversion results. Comput. Geosci. 28, 1037–1040.
Lisle, R.J., Srivastava, D.C., 2004. Test of the frictional reactivation theory for faults and validity of fault-slip analysis. Geology 32, 569–572. https://doi.org/10.1130/G20408.1.
Lund Snee, J.E., Zoback, M.D., 2020. Multiscale variations of the crustal stress field throughout North America. Nat. Commun. 11. https://doi.org/10.1038/s41467-020-15841-5.
Main, I., Irving, D., Musson, R., Reading, A., 1999. Constraints on the frequency-magnitude relation and maximum magnitudes in the UK from observed seismicity and glacio-isostatic recovery rates. Geophys. J. Int. 137, 535–550. https://doi.org/10.1046/j.1365-246X.1999.00796.x.
Marrow, P.C., Walker, A.B., 1988. Lleyn earthquake of 1984 July 19: aftershock sequence and focal mechanism. Geophys. J. Int. 92, 487–493. https://doi.org/10.1111/j.1365-246X.1988.tb00011.x.
Mckay, L., Lunn, R.J., Shipton, Z.K., Pytharouli, S., Roberts, J.J., 2021. Do intraplate and plate boundary fault systems evolve in a similar way with repeated slip events? Earth Planet Sci. Lett. 559, 116757. https://doi.org/10.15129/21271686-f115.
Moeck, I., Kwiatek, G., Zimmermann, G., 2009. Slip tendency analysis, fault reactivation potential and induced seismicity in a deep geothermal reservoir. J. Struct. Geol. 31, 1174–1182. https://doi.org/10.1016/j.jsg.2009.06.012.
Morris, A., Ferrill, D.A., Henderson, D.B., 1996. Slip-tendency analysis and fault reactivation. Geology 24, 275–278.
Mosca, I., Sargeant, S., Baptie, B., Musson, R.M.W., Pharaoh, T.C., 2022. The 2020 national seismic hazard model for the United Kingdom. Bull. Earthq. Eng. 20, 633–675. https://doi.org/10.1007/s10518-021-01281-z.
Muir-Wood, R., 2000. Deglaciation seismotectonics: a principal influence on intraplate seismogenesis at high latitudes. Quat. Sci. Rev. 19, 1399–1411.
Musson, R., Sargeant, S., 2007. Eurocode 8 seismic hazard zoning maps for the UK seismology and geomagnetism programme. British Geological Survey 70. Technical Report CR/07/125.
Musson, R.M.W., 2012. Interpreting intraplate tectonics for seismic hazard: a UK historical perspective. J. Seismol. 16, 261–273. https://doi.org/10.1007/s10950-011-9268-1.
Musson, R.M.W., 2007. British earthquakes. PGA (Proc. Geol. Assoc.) 118, 305–337. https://doi.org/10.1016/S0016-7878(07)80001-0.
Musson, R.M.W., 1997. Seismic hazard studies in the U.K.: source specification problems of intraplate seismicity. Nat. Hazards 15, 105–119.
ONR, 2018. ONR expert panel on natural hazards analysis of seismic hazards for nuclear sites sub-panel on seismic hazards. Expert Panel Paper No: GEN-SH-EP-2016-1.
Peacock, D.C.P., Kley, J., Leiss, B., 2025. Using fault maps for preliminary screening of areas for underground storage of radioactive waste or for geothermal energy. Geoenergy 2024-032. https://doi.org/10.1144/geoenergy2024-032.
Powers, P.M., Jordan, T.H., 2010. Distribution of seismicity across strike-slip faults in California. J. Geophys. Res. Solid Earth 115, B05305. https://doi.org/10.1029/2008JB006234.
Rajabi, M., Lammers, S., Heidbach, O., 2025. WSM database description and guidelines for analysis of horizontal stress orientation from borehole logging. World Stress Map Technical Report 25-01, GFZ Helmholtz Centre for Geosciences. https://doi.org/10.48440/wsm.2025.001.
Röckel, L., Ahlers, S., Müller, B., Reiter, K., Heidbach, O., Henk, A., Hergert, T., Schilling, F., 2022. The analysis of slip tendency of major tectonic faults in Germany. Solid Earth 13, 1087–1105. https://doi.org/10.5194/se-13-1087-2022.
Sandiford, M., Wallace, M., Coblentz, D., 2004. Origin of the in situ stress field in south-eastern Australia. Basin Res. 16, 325–338. https://doi.org/10.1111/j.1365-2117.2004.00235.x.
Stewart, I.S., Firth, C.R., 2000. Neotectonics of the United Kingdom: a Review of Existing Information. Contractors Report to NIREX by Neotectonics Research Centre, Department of Geography and Earth Sciences. Brunel University.
Townend, J., Zoback, M., 2000. How faulting keeps the crust strong. Geology 28, 399–402.
Tozer, B., Sandwell, D.T., Smith, W.H.F., Olson, C., Beale, J.R., Wessel, P., 2019. Global bathymetry and topography at 15 arc sec: SRTM15+. Earth Space Sci. 6, 1847–1864. https://doi.org/10.1029/2019EA000658.
Trodd, H., Warburton, P., Pooley, C.I., 1985. The great British earthquake of 1984 seen from afar. Geophys. J. Int. 83, 809–812.
Tuttle, M.P., Schweig, E.S., Sims, J.D., Lafferty, R.H., Wolf, L.W., Haynes, M.L., 2002. The earthquake potential of the new Madrid seismic zone. Bull. Seismol. Soc. Am. 92, 2080–2089.
Williams, J.D.O., Gent, C.M.A., Fellgett, M.W., Gamboa, D., 2018. Impact of in situ stress and fault reactivation on seal integrity in the east Irish sea basin, UK. Mar. Petrol. Geol. 92, 685–696. https://doi.org/10.1016/j.marpetgeo.2017.11.030.
Wiprut, D., Zoback, M.D., 2002. Fault reactivation, leakage potential, and hydrocarbon column heights in the northern north sea. In: Koestler, A.G., Hunsdale, R. (Eds.), Hydrocarbon Seal Quantification. NPF Special Publication, pp. 203–219.
Woodcock, N.H., Strachan, R.A., 2012. Geological History of Britain and Ireland, second ed. John Wiley and Sons.
Yukutake, Y., Takeda, T., Yoshida, A., 2015. The applicability of frictional reactivation theory to active faults in Japan based on slip tendency analysis. Earth Planet Sci. Lett. 411, 188–198. https://doi.org/10.1016/j.epsl.2014.12.005.
Ziegler, M.O., Heidbach, O., 2019. Matlab script Stress2Grid v1.1. GFZ Data Services.
Zoback, M. Lou, Zoback, M.D., 1989. Tectonic Stress Field of the Continental United States, 172. Geological Society of America Memoir, pp. 523–539.